RSC Advances

RSC Publishing

PAPER

# A density functional study of phosphorus-doped gold clusters: $Au_nP^-$ ($n$ = 1–8)†

Cite this: *RSC Adv.*, 2013, **3**, 24492

Kang-Ming Xu,[a] Teng Huang,[a] Hui Wen,[a] Yi-Rong Liu,[a] Yan-Bo Gai,[a] Wei-Jun Zhang*[ab] and Wei Huang*[ab]

Received 26th July 2013
Accepted 9th October 2013

DOI: 10.1039/c3ra43938k

**www.rsc.org/advances**

The geometries of phosphorus-doped gold clusters, $Au_nP^-$ ($n$ = 1–8), have been investigated using different density functionals and basis sets. B3LYP and PBE functionals with 4 basis sets (aug-cc-pVDZ, 6-311++G**, CRENBL ECP and LANL2DZ ECP) are chosen for geometry optimisation. Many low-lying structures are obtained for anionic $Au_nP^-$ clusters. For $Au_nP^-$ ($n$ = 1–7) clusters, each level gives the same global minimum structure. It is found that the evolutionary path of phosphorus-doped gold clusters differs from that of pure gold clusters. Phosphorus atoms induce changes in the structure of pure gold clusters in small cluster sizes. Various 2D–3D structures of doped clusters are also investigated. Clusters with an odd number of gold atoms tend to yield planar 2D structures, while those with an even number of gold atoms tend to yield 3D structures.

## 1. Introduction

The element gold has unique properties that are strongly influenced by relativistic effects.[1–3] It is well known that gold nano-clusters exhibit catalytic properties, as first reported by Haruta,[4] after which point the structures of gold nano-clusters received significant attention.[1–3,5] A series of experimental and theoretical studies have been conducted on the distinctive structures and interesting properties of pure gold clusters in the small-to-medium size range.[6–23] Gold clusters doped with heterogeneous species also have been widely investigated following expectations that varying the dopant alters the size and shape of the clusters in addition to tailoring the properties of the nano-clusters.[24–38]

The study of phosphorus-doped gold clusters has received significant attention, motivated in part by the goal to understand the fascinating properties of materials in general, such as semiconductors and unique optical properties.[39,40] There have been a number of experimental[41–46] and theoretical[47–51] investigations of the reactivity of gold clusters doped with phosphorus.

Jeitschko and Moller[41] studied the Au–Au interaction in the crystal structure of the well-known $Au_2P_3$ structure. Eschen and Jeitschko[42] reported the network crystal structure of $Au_2MP_2$ (M = Pb, Tl, Hg) in three dimensions with condensed 8-membered $Au_2P_6$ and 10-membered $Au_4P_6$ rings. Weizer and Fatemi[43] reported the contact resistance of a $Au_2P_3$ layer, found to be very sensitive to the growth rate of the interfacial $Au_2P_3$ layer. Henkes *et al.*[44] reported on $Au_2P_3$ and other metal phosphides synthesised using a hot solvent of trioctylphosphine (TOP). The study of the generation of $Au_nP_m^{\pm}$ based on the use of a Nd:YAG (532 nm) laser was reported by Zheng and co-workers.[45] Recently, Panyala *et al.*[46] also studied $Au_nP_m^{\pm}$ clusters using laser ablation coupled with TOF-MS.

In contrast, there have been relatively few theoretical studies of the structural and bonding properties of Au–P clusters using different calculation methods, such as *ab initio* and density functional theory (DFT).[48–51] Theoretical studies have been undertaken by Wen *et al.* on the electronic structures of $Au_2MP_2$ (M = Pb, Tl, Hg).[47] Similar results have been reported by Eschen and Jeitschko[42] on the network crystal structure of $Au_2MP_2$ (M = Pb, Tl, Hg). Li *et al.*[48] studied the geometries, stabilities, and electronic properties of neutral $Au_nP_2$ ($n$ = 1–8) clusters using an *ab initio* method based on DFT at the PW91PW91 level. Zhao *et al.*[49] reported findings of neutral $Au_{12}$ clusters doped with the secondary periodic elements based on DFT. The atomic and electronic structure of $Au_5M$ (M = Na, Mg, Al, Si, P, and S)[51] and $M@Au_6$ (M = Al, Si, P, S, Cl, and Ar)[50] clusters have been investigated using DFT with the scalar relativistic effective core potential basis set. However, to the best of our knowledge, there have been no systematic investigations of anionic phosphorus-doped gold clusters in the reported literature.

In the current article, we report a density functional study of a series of small gold clusters doped with a single phosphorus atom ($Au_nP^-$ ($n$ = 1–8)). We chose this size range specifically to probe the manner in which isoelectronic substitutions affect the structures of pure gold clusters. The low-lying structures of $Au_3P^-$ and $Au_4P^-$ clusters are significantly different with the

[a]*Laboratory of Atmospheric Physico-Chemistry, Anhui Institute of Optics and Fine Mechanics, Chinese Academy of Sciences, Hefei, Anhui 230031, China. E-mail: huangwei6@ustc.edu.cn; wjzhang@aiofm.ac.cn*

[b]*School of Environmental Science and Optoelectronic Technology, University of Science and Technology of China, Hefei, Anhui 230026, China*

† Electronic supplementary information (ESI) available. See DOI: 10.1039/c3ra43938k

pure gold clusters of $Au_4^-$ and $Au_5^-$. Additionally, clusters with an odd number of gold atoms tend to arrange in planar 2D structures, while those with an even number of gold atoms tend to form 3D structures.

## 2. Theoretical methods

The basin-hopping (BH) global searching method[52–55] coupled with DFT was employed to search for low-lying isomers of phosphorus-doped clusters of the type $Au_nP^-$ ($n$ = 1–8). Randomly produced structures of each species were used as the initial inputs for the BH search program, and 200 rudely low-lying isomers were generated after 200–300 BH moves. Considering the inevitable errors of the DFT methods when applied to total energy calculations, several addition techniques were chosen for DFT optimisation, including generalised gradient approximation (GGA) in the Perdue–Burke–Ernzerhof (PBE),[56] *hybrid* generalised gradient approximation (*hybrid*-GGA) in the Becke 3-parameter exchange and Lee-Yang-Parr correlation (B3LYP)[57–59] functional forms coupled with four basis sets, *i.e.*, aug-cc-pVDZ, 6-311++G**, CRENBL ECP and LANL2DZ ECP (PBE/aug-cc-pVDZ, PBE/6-311++G**, PBE/CRENBL ECP, PBE/LANL2DZ ECP, B3LYP/aug-cc-pVDZ, B3LYP/6-311++G**, B3LYP/CRENBL ECP and B3LYP/LANL2DZ ECP; 8 levels), respectively; all approaches were implemented in the NWCHEM 5.1.1 software package.[60,61]

The relative energy of the top-10 isomers was chosen for single-point energy calculations at the PBE0[62]/aug-cc-pVTZ, PBE0/6-311++G(3df,3pd), PBE0/CRENBL ECP, PBE0/LANL2DZ ECP, B3LYP/aug-cc-pVTZ, B3LYP/6-311++G(3df,3pd), B3LYP/CRENBL ECP and B3LYP/LANL2DZ ECP levels of theory for the phosphorus atom. By considering the strong relativistic effects of the gold atom, CRENBL ECP basis set and the spin–orbit (SO) effects[63] were carefully selected for the gold atom to achieve quantitative agreement between the experimental and theoretical PES spectra.[54,64–68]

The theoretical photoelectron spectra of the selected low-lying isomers were simulated for comparison with different levels of functional and basic sets to further identify the $Au_nP^-$ ($n$ = 2–8) clusters. The first vertical detachment energies (VDEs) of the anion clusters were calculated as the difference between the energies of the neutral and anion species of each isomer. The binding energies of all deeper occupied orbits were then added to the first VDE to simulate the detachment features of the inner electrons as a line spectrum. Each line of the spectrum obtained was then fitted with a Gaussian width of 0.04 eV to yield the continuous spectra.

## 3. Results and discussion

In this section, we focus on the structures of $Au_nP^-$ ($n$ = 2–8) at 8 levels of theoretical methods, in addition to the theoretically simulated PES spectra, which show the VDEs and LUMO–HOMO gaps for all the low-lying isomers of each species. For the integrity of the species studied, $AuP^-$ is also discussed based on the bond length at different levels of theory. Then, we try to give the possible evolutionary process of the phosphorus-doped gold clusters. Different theoretical methods were used for comparison due to the lack of experimental data. We list the results obtained at the PBE0/6-311++G(3df,3pd) SO//PBE/6-31++G** level of theory, which was verified to be the best-suited for the species in our study. Other results are listed in the ESI.†

### 3.1 Low-lying structures

**$AuP^-$.** $AuP^-$ has only one dumbbell structure. Fig. 1 gives the different bond lengths of the anionic Au–P cluster at 8 levels of theory. The length of the Au–P bond in our study ranged from 2.288 Å (at B3LYP/aug-cc-pVDZ level) to 2.760 Å (at PBE/CRENBL ECP level), which is consistent with the reports of former work.[49–51]

**$Au_2P^-$.** The 3 possible isomers of $Au_2P^-$ and its energy order at the PBE0/CRENBL ECP level of theory are listed in Table 1, while the results obtained from other levels of theory are presented in Table S1 (ESI†). The global minimum of $Au_2P^-$ is the $C_{2v}$ symmetry configuration, which possesses the same geometric structure as the water molecule and $Au_2X^-$ (X = Mg, Al, Si).[69–72] The second isomer, a $C_{\infty h}$ structure with the phosphorus atom residing at the edge of a Au–Au bond, has a relatively large energy difference relative to Isomer 1. However, for the B3LYP/CRENBL ECP and B3LYP/LANL2DZ ECP levels of theory, the energy difference is only 0.077 eV and 0.064 eV within an "isomer-coexistence interval" of 0.1 eV, which coincides with an estimate of the accuracy of the DFT method for gold clusters (deduced from a comparison between the recent mobility measurements and theoretical calculations[7]). The $D_{\infty h}$ isomer exhibits a large energy difference, given by the PBE0/aug-cc-pVTZ, B3LYP/aug-cc-pVTZ, B3LYP/6-311++G(3df,3pd) and B3LYP/CRENBL ECP methods, and has little possibility of being the most stable isomer.

**$Au_3P^-$.** The isomers of $Au_3P^-$ are shown in Table 1 at the PBE0/CRENBL ECP level of theory, and the results from other levels of theory are shown in Table S2 (ESI†). The global minimum is an axe-like structure ($C_s$) with an additional gold atom added to the gold atom of either side of $Au_2P^-$. Isomer 2 is a triangular pyramidal structure ($C_{3v}$) at all levels of theory investigated except for the B3LYP/CRENBL ECP level, and its

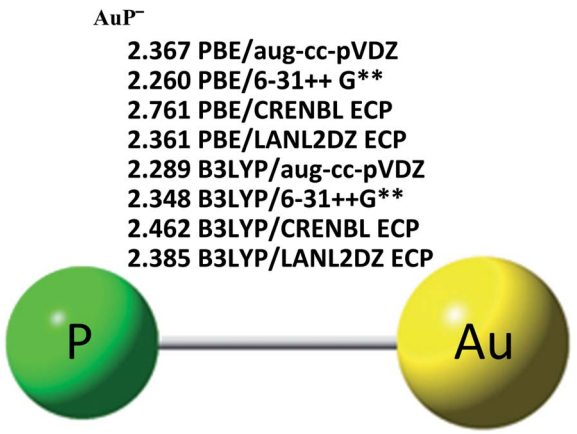


**Fig. 1** The molecular geometry of $AuP^-$ and its bond lengths at 8 levels of theory. All bond lengths are in Å.

energy difference compared with Isomer 1 is a little larger, exceeding the "isomer-coexistence interval" of 0.1 eV. The zigzag isomer and tower isomer, both of which are possible low-lying isomers for the $Au_4^-$ cluster (Fig. S1†), also were found, but the conformations are not the global minima in our study.[7,8,73]

Isomer 1 shows the same geometry as $Au_3S^-$, while the global minima of $Au_3X^-$ (X = Na, Mg, Al, Si) are similar to Isomer 3 of $Au_3P^-$; additionally, these structures all vary from the low-lying isomers of pure $Au_4^-$.[7,8,38,69–74]

**$Au_4P^-$.** The low-lying isomers of $Au_4P^-$ are shown in Tables 1 and S3 (ESI†). For $Au_4P^-$, the global minimum is a "rake-shaped"

**Table 1** The possible structural isomers, relative energies and molecular geometry symmetries of the low-lying isomer of $Au_nP^-$ ($n$ = 1–8) at the PBE0/CRENBL ECP level of the theory[a]

| | Structures, energies (eV) & geometric symmetries | | | | |
|---|---|---|---|---|---|
| Species | Isomer 1 | Isomer 2 | Isomer 3 | Isomer 4 | Isomer 5 |
| $AuP^-$ |  0.000 $C_{\infty h}$ | | | | |
| $Au_2P^-$ | 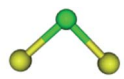 0.000 $C_{2v}$ | 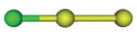 0.154 $C_{\infty h}$ |  1.103 $D_{\infty h}$ | | |
| $Au_3P^-$ | 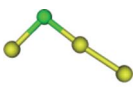 0.000 $C_s$ | 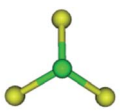 0.639 $C_{3v}$ |  0.664 $C_{2v}$ |  0.929 $C_1$ | |
| $Au_4P^-$ | 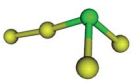 0.000 $C_s$ | 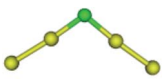 0.727 $C_{2v}$ | 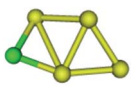 0.821 $C_1$ | 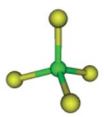 1.035 $T_d$ | |
| $Au_5P^-$ | 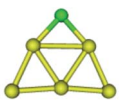 0.000 $C_{2v}$ | 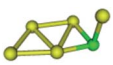 0.585 $C_1$ | 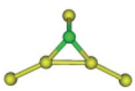 0.674 $C_s$ | 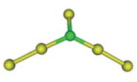 0.704 $C_s$ | 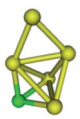 0.737 $C_{2v}$ |
| $Au_6P^-$ | 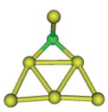 0.000 $C_s$ |  0.753 $C_{2v}$ | 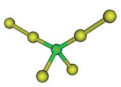 0.833 $C_{2v}$ | 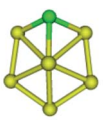 0.875 $C_{2v}$ | 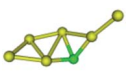 0.878 $C_1$ |
| $Au_7P^-$ | 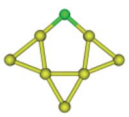 0.000 $C_{2v}$ | 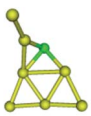 0.313 $C_1$ | 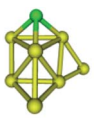 0.326 $C_1$ | 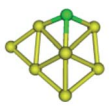 0.392 $C_1$ | 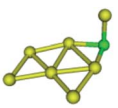 0.401 $C_1$ |
| $Au_8P^-$ | 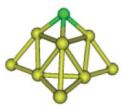 0.000 $C_s$ | 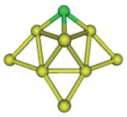 0.034 $C_s$ | 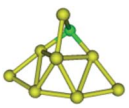 0.152 $C_s$ | 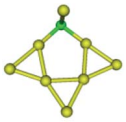 0.153 $C_s$ | 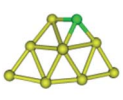 0.342 $C_1$ |

[a] The top-5 isomers are ranked according to their relative energies for $Au_nP^-$ ($n$ = 5–8), while the top-4 isomers for $Au_nP^-$ and $Au_nP^-$, as well as the top-3 isomers for $Au_2P^-$ and the only isomer of $AuP^-$.

structure ($C_s$). This structure can be envisioned by the addition of an additional gold atom to the triangular pyramidal structure of $Au_3P^-$. As seen in Table S3,† the second isomer obtained using the aug-cc-pVTZ and 6-311++G(3df,3pd) basis sets differs from that using the CRENBL ECP and LANL2DZ ECP basis sets. A high-symmetry structure ($T_d$) of $Au_4P^-$ with lower energies is found at the PBE0/aug-cc-pVTZ, PBE0/6-311++G(3df,3pd), B3LYP/aug-cc-pVTZ, B3LYP/6-311++G(3df,3pd) levels of theory, although this structure still shows a significant energy difference (greater than 0.7 eV) relative to the global minimum. In contrast, a "Λ-shaped" structure occupies the second place at the levels of PBE0/CRENBL ECP, PBE0/LANL2DZ ECP, B3LYP/CRENBL ECP, and B3LYP/LANL2DZ ECP. Both the $T_d$ and $C_{2v}$ structures have relatively higher energy values than the lowest-energy rake-like structure ($C_s$). A structure similar to that of the pure $Au_5$ anionic cluster[8] was found only at the PBE0/CRENBL ECP level and was not identified as the most stable isomer for $Au_4P^-$.

It is an intriguing result that the low-lying isomers of secondary periodic elements doped with 4 gold atoms vary among each other and differ from the pure $Au_5^-$ cluster, as well.[38,68–71,73]

**$Au_5P^-$.** The top-5 low-lying structures of $Au_5P^-$ are shown in Tables 1 and S4 (ESI†), respectively. The global minimum is a planar-quasi-triangular structure ($C_{2v}$) with a phosphorus atom substituting the vertex gold atom of the $Au_6^-$ cluster, which was previously reported by Häkkinen.[8,73] As seen in Table S4,† two isomers are placed in the second order, which is a $C_1$ structure with one dangling gold atom bonded to a phosphorus atom at the PBE0/CRENBL ECP and PBE0/LANL2DZ ECP levels and a quasi-planar structure ($C_s$) at the remaining 6 levels. The $C_s$ isomer has a relative small energy difference relative to Isomer 1. They are 0.031 eV at the B3LYP/aug-cc-pVTZ level and 0.032 eV at the B3LYP/6-311++G(3df,3pd) level, respectively. The $C_s$ isomer has not been reported for pure gold clusters but may be the possible stable isomer for $Au_5P^-$. Isomer 2 of $Au_5P^-$, as shown in Table 1, has a higher energy relative to Isomer 1, indicating the low possibility for this to be the most stable structure in our study.

The low-lying isomer of $Au_5P^-$ is similar to the global minimum of the pure $Au_6^-$ cluster, which also shares similarities with $Au_5S^-$, and the same structure of $Au_5Mg^-$ with the single Mg atom locating the impurity on one side of the equilateral triangle structure shows a relative 2.46 eV higher than the low-lying isomer of the species.[38,69]

**$Au_6P^-$.** For $Au_6P^-$, the global minimum is Isomer 1, as shown in Table 1, with a Au atom dangling at the location of the phosphorus atom of the $Au_5P^-$ planar structure. This $C_s$ structure is similar to the minor isomer of $Au_7^-$, which consists of a triangular $Au_6$ unit and a dangling Au atom reported by Huang *et al.*,[54] who confirmed the existence of this isomer using experimental and theoretical methods. The same structure was not found in gold clusters doped with the same periodic elements of phosphorus.[69,70,75]

A saddle-like structure at the PBE0/aug-cc-pVTZ, PBE/6-311++G(3df,3pd), B3LYP/aug-cc-pVTZ, B3LYP/6-311++G(3df,3pd), B3LYP/CRENBL ECP, B3LYP/LANL2DZ ECP six levels is placed in the second rank, while the global minimum difference to Isomer 1 is the $C_{2v}$ structure at the PBE0/CRENBL ECP, PBE0/LANL2DZ ECP levels with 0.171 eV and 0.173 eV, respectively (see Table S5 (ESI†)). The energy difference between Isomer 1 and Isomer 2 exceeds the "isomer-coexistence interval," thus Isomer 1 is the most stable structure of $Au_6P^-$ and may be the only structure.

Another unique structure that should be mentioned is the hexagonal structure ($C_{2v}$) listed in Table 1 at the PBE0/CRENBL ECP level with an energy value that is 0.875 eV higher than that of Isomer 1. This significant energy difference indicates that the structure is unlikely to be the most stable structure.

The global minimum of anionic $Au_6P^-$ cluster differs from the neutral one.[50] It also should be noted that the anion and neutral structures may be significantly different from each other due to the interaction of one more electron with respect to the stability of the cluster.[38,73]

**$Au_7P^-$.** As seen in Table 1, the global minimum (Isomer 1) is a planar $C_{2v}$ structure at the PBE0/CRENBL ECP level, as well as at other levels of the theory (see Table S6 (ESI†)). Isomer 1 is a "kite-like" structure, similar to the "star-like" structure of $Au_8^-$ in which one gold atom is substituted by a phosphorus atom.[7,8,54]

A structure ($C_s$) with two gold atoms dangling on the triangular $Au_6$ unit also can be found in Table S6 (ESI†). The energy difference between the structure mentioned relative to Isomer 1 is 0.081 eV at the B3LYP/aug-cc-pVTZ level and 0.095 eV at the B3LYP/6-311++G(3df,3pd) level. This conformation also might be the stable isomer of $Au_7P^-$ due to the energy difference within an "isomer-coexistence interval" of 0.1 eV. Another phenomenon should be noted here, namely, that Isomer 2 of $Au_7P^-$ (Table 1) has a mirror structure with the dangling gold atoms bonded to the right side of the 1$^{st}$ gold atom (the number of gold atoms is labelled in Fig. 10). Isomers 3–5 in Table 1 are unlikely to be the stable isomer in our study because each has a significant energy difference relative to Isomer 1.

**$Au_8P^-$.** In contrast to the clusters discussed previously, $Au_8P^-$ may have 3 distinct minima at the different levels, as shown in Table S7 (ESI†). To describe the structure more clearly, we label the gold atoms of $Au_8P^-$ as shown in Fig. 9. As shown in Table S7,† when coupling the B3LPY *hybrid* functional theory with the four selected basis sets (aug-cc-pVTZ, 6-311++G(3df,3pd), CRENBL ECP and LANL2DZ ECP), the global minimum can be considered as a structure in which one extra gold atom dangles off the phosphorus atom of the planar $Au_7P^-$ structure, making it a 3D structure. The global minimum with the PBE functional varies from the structure obtained with the B3LYP hybrid functional. For example, in the global minimum at the PBE0/aug-cc-pVTZ and PBE0/6-311++G(3df,3pd) levels, the dangling gold atom (5$^{th}$) bonds with inner-ring gold atoms (1$^{st}$ and 3$^{rd}$); however, for that at the PBE0/CRENBL ECP and PBE0/LANL2DZ ECP levels, the 5$^{th}$ gold atom also connects with the 4$^{th}$ gold atom of $Au_8P^-$. The global minimum in Table 1 is similar with the structure of the pure gold $Au_9^-$ cluster in which a phosphorus atom substitutes one outer-ring gold atom of the "star-like" structure and bonds with the central gold atom.[7,8]

Isomer 3 of the PBE0/CRENBL ECP functional/basic set also could be the stable structure of the species because the energy of the structure is 0.057 eV at the PBE0/aug-cc-pVTZ theory level.

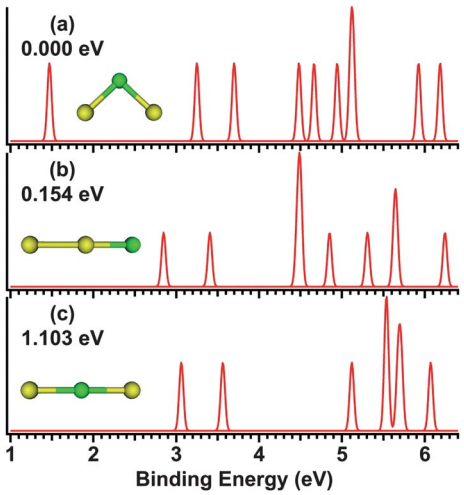


**Fig. 2** Simulated photoelectron spectra of $Au_2P^-$ at the PBE0/CRENBL ECP SO//PBE/CRENBL ECP level of theory.

### 3.2 Simulated photoelectron spectra

Fig. 2 shows the simulated photoelectron spectra of $Au_2P^-$. The global minimum (Isomer 1) specifies a lower vertical detachment energy (VDE) and a larger LUMO–HOMO gap than that of the other two isomers. This suggests that the neutral structure of $Au_2P^-$ ($C_{2v}$) is more stable than the anionic structure.

Isomer 1 of $Au_3P^-$ has three adjacent peaks at the PBE0/CRENBL ECP SO//PBE/CRENBL ECP level (Fig. 3). Isomer 2 has a lower VDE than the other structures but is not the global minimum. Isomer 3 has a relatively higher first VDE and LUMO–HOMO gap; similar findings were recorded for Isomer 4.

The simulated photoelectron spectra of $Au_4P^-$ are shown in Fig. 4. The VDE of Isomer 1 of $Au_4P^-$ is 3.42 eV at the PBE0/CRENBL ECP SO//PBE/CRENBL ECP level. The high detachment energy indicates that the global minimum can exist stably. Isomer 2, which exhibits a significant energy difference of 0.727

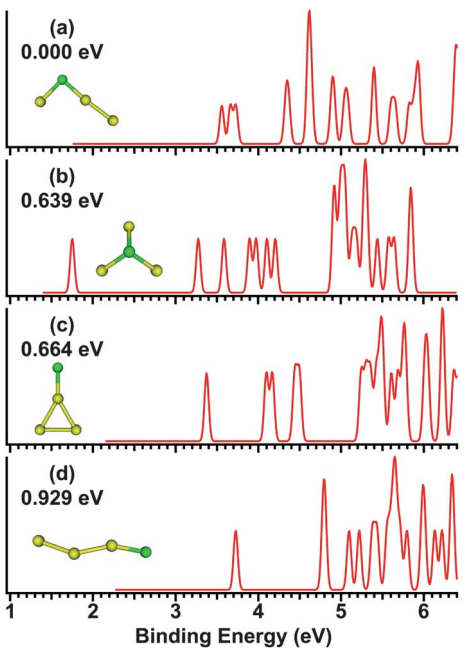


**Fig. 3** Simulated photoelectron spectra of $Au_3P^-$ at the PBE0/CRENBL ECP SO//PBE/CRENBL ECP level of theory.

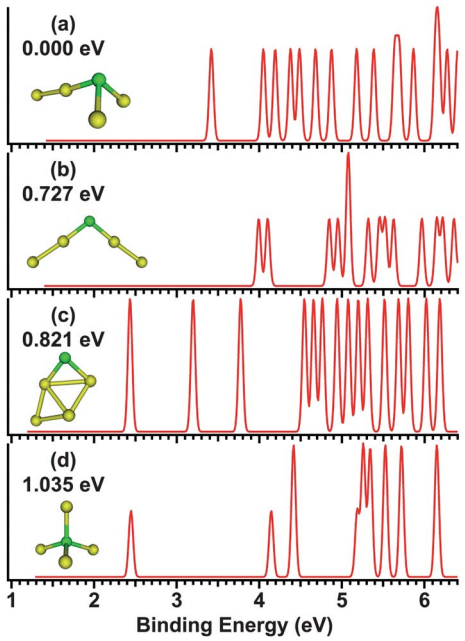


**Fig. 4** Simulated photoelectron spectra of $Au_4P^-$ at the PBE0/CRENBL ECP SO//PBE/CRENBL ECP level of theory.

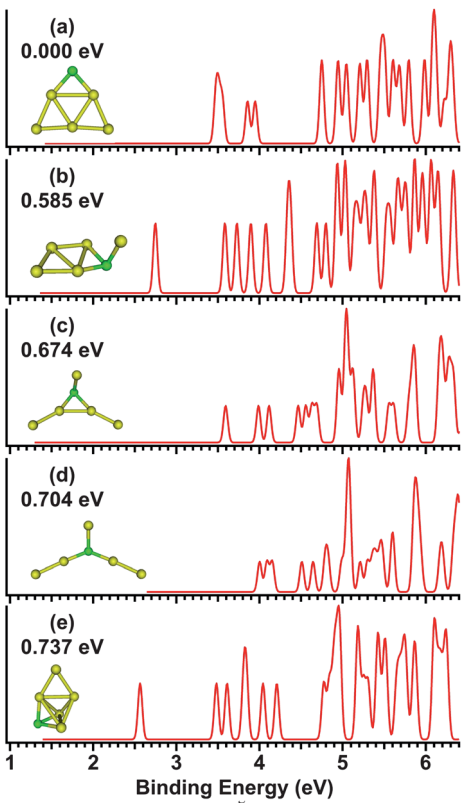


**Fig. 5** Simulated photoelectron spectra of $Au_5P^-$ at the PBE0/CRENBL ECP SO//PBE/CRENBL ECP level of theory.

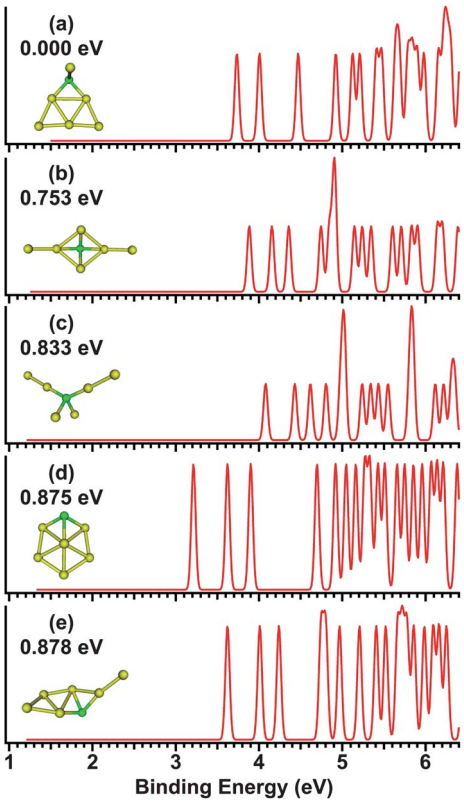


**Fig. 6** Simulated photoelectron spectra of $Au_6P^-$ at the PBE0/CRENBL ECP SO//PBE/CRENBL ECP level of theory.

eV, also has a high VDE, while Isomer 3 and Isomer 4 have lower VDEs than the two isomers mentioned above. Isomer 4, which is a high-symmetry structure ($T_d$), yields a simpler spectrum than those of the other isomers. Additionally, the significant LUMO–HOMO gap of Isomer 4 indicates that Isomer 4 has a stable ground state.

Fig. 5–8 show the simulated photoelectron spectra of the top-5 isomers of $Au_nP^-$ ($n = 5$–8) at the PBE0/CRENBL ECP SO//PBE/CRENBL ECP level of theory. Fig. S5–S8† compare the spectra of the global minimum of $Au_nP^-$ ($n = 5$–8) obtained at all 8 levels of theory, while the corresponding simulated VDEs are listed in Table 2. As seen, different levels show almost the same peak shape, although they present different VDEs. The first peak of Isomer 1 of $Au_5P^-$ varies at different levels of the theory (Fig. S5†). The VDE of Isomer 1 is in the range from 3.41 eV to 3.50 eV. The VDE of Isomer 2 is significantly lower than that of Isomer 1, which means that the structure more easily loses an electron relative to Isomer 1. Isomer 3 varies from Isomer 4 due to the additional bond connecting two gold atoms. This creates the distinct electron distribution of the structure, as well as its unique photoelectron spectra. Fig. 6 and 7 show the spectra of the top-5 low-lying isomers of $Au_6P^-$ and $Au_7P^-$, respectively. For the $Au_8P^-$ cluster, the simulated photoelectron spectra of the 3 global minima discussed in Section 3.1 are listed in Fig. 8. Isomer 1 has one more bond than Isomer 2, which leads to splitting of the second peak of Isomer 1 into two peaks.

As seen from Fig. S2–S8,† except for $Au_2P^-$, the VDEs are all larger than 3 eV, for clusters of $Au_3P^-$ through $Au_8P^-$.

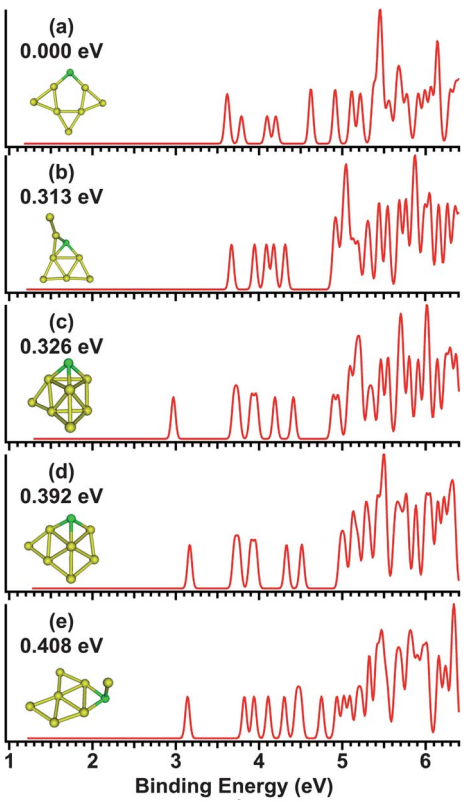


**Fig. 7** Simulated photoelectron spectra of $Au_7P^-$ at the PBE0/CRENBL ECP SO//PBE/CRENBL ECP level of theory.

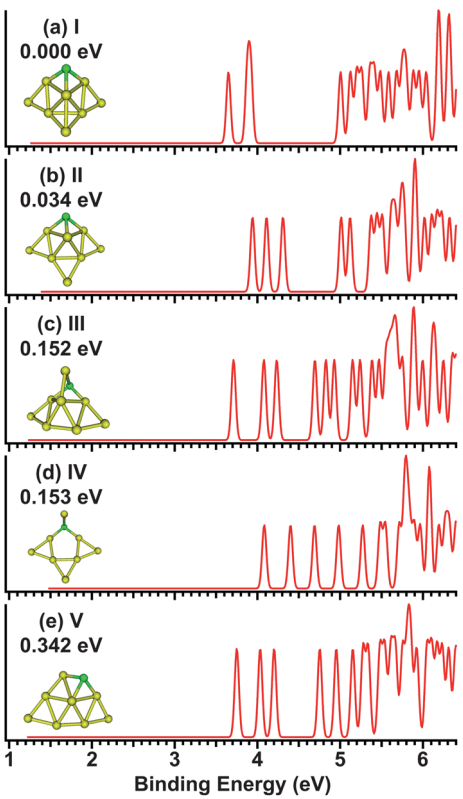


**Fig. 8** Simulated photoelectron spectra of $Au_8P^-$ at the PBE0/CRENBL ECP SO//PBE/CRENBL ECP level of theory.

**Table 2** The theoretical simulated VDEs from the anion photoelectron spectra of the low-lying isomers of $Au_nP^-$ ($n$ = 2–8) at the 8 levels of theory[a]

| | | VDE (eV) | | | | | | | |
|---|---|---|---|---|---|---|---|---|---|
| Species | Isomers | a | b | c | d | e | f | g | h |
| $Au_2P^-$ | 1 | 1.67 | 1.65 | 1.47 | 1.49 | 1.81 | 1.79 | 1.59 | 1.61 |
| $Au_3P^-$ | 1 | 3.49 | 3.47 | 3.56 | 3.57 | 3.52 | 3.50 | 3.57 | 3.58 |
| $Au_4P^-$ | 1 | 3.37 | 3.37 | 3.42 | 3.41 | 3.48 | 3.48 | 3.50 | 3.51 |
| $Au_5P^-$ | 1 | 3.43 | 3.41 | 3.47 | 3.48 | 3.46 | 3.45 | 3.49 | 3.50 |
| $Au_6P^-$ | 1 | 3.49 | 3.73 | 3.73 | 3.51 | 3.62 | 3.85 | 3.85 | 3.63 |
| $Au_7P^-$ | 1 | 3.55 | 3.53 | 3.61 | 3.61 | 3.58 | 3.57 | 3.63 | 3.63 |
| $Au_8P^-$ | 1 | 3.68 | 3.59 | 4.08 | 3.74 | 3.79 | 3.80 | 4.18 | 3.85 |
| | 2 | 3.89 | 3.70 | 3.94 | 3.73 | 3.80 | 3.80 | 4.04 | 3.83 |
| | 3 | 3.59 | 3.59 | 3.65 | 3.65 | 3.95 | 3.87 | 3.74 | 3.75 |

[a] a: PBE0/aug-cc-pVTZ SO//PBE/aug-cc-pVDZ; b: PBE0/6-311++G(3df,3pd) SO//PBE/6-31++G**; c: PBE0/CRENBL ECP SO//PBE/CRENBL ECP; d: PBE0/LANL2DZ ECP SO//PBE/LANL2DZ ECP; e: B3LYP/aug-cc-pVTZ SO//B3LYP/aug-cc-pVDZ; f: B3LYP/6-311++G(3df,3pd) SO//B3LYP/6-31++G**; g: B3LYP/CRENBL ECP SO//B3LYP/CRENBL ECP; h: B3LYP/LANL2DZ ECP SO//B3LYP/LANL2DZ ECP.

Additionally, it can be seen that each cluster with even numbers of gold atoms ($Au_nP^-$, $n$ = 2, 4, 6, 8) exhibits a single first peak and a relative larger LUMO–HOMO energy gap. The gaps tend to become smaller while the VDEs become larger, as the number of gold atoms increases. The clusters with odd numbers of gold atoms ($Au_nP^-$, $n$ = 3, 5, 7) have more complicated photoelectron spectra than the even-numbered clusters: the first peak of each odd-numbered cluster splits into double or triple peaks. This result may be due to the differences in the electron multiplicity of the species, *i.e.*, $Au_nP^-$ ($n$ = 2, 4, 6, 8) is a singlet and $Au_nP^-$ ($n$ = 3, 5, 7) is a doublet.

### 3.3 Evolution of the structures

To identify a rule that governs the growth of single phosphorus-doped gold clusters from small to medium sizes, we investigated the evolution of the clusters by choosing the most likely isomers of the $Au_nP^-$ ($n$ = 1–8) species, as calculated by the 8 levels mentioned above. Fig. 9 shows the possible evolutionary path from a small cluster to a medium cluster.

The $AuP^-$ cluster, as the initial unit, has only one dumbbell ($C_{\infty h}$) structure. This dumbbell structure adds a Au atom to the side at which the phosphorus atom side is bonded, forming a $C_{2v}$ structure, which is the most stable structure for $Au_2P^-$, according to our study.

Two possible paths from $Au_2P^-$ to $Au_3P^-$ arise. $Au_2P^-$ (I) tends to add a 3rd gold atom to the gold atom side to form $Au_3P^-$. Alternatively, the gold atom can combine with the phosphorus atom of $Au_2P^-$ (II) to form $Au_3P^-$.

The axe-like isomer of $Au_3P^-$ can be envisioned as the rhombus isomer of $Au_4^-$, where one gold atom is replaced by one phosphorus atom, while a Au–Au bond is simultaneously broken.

Two isomers of $Au_4P^-$ are shown in Fig. 9. $Au_4P^-$ (I), which has a 3D structure, is formed by the addition of another initial gold atom to the phosphorus atom of $Au_3P^-$ ($C_s$). In contrast, $Au_4P^-$ (II) is obtained by the addition of one more gold atom to $Au_3P^-$; this atom binds with each of the gold atoms already present, forming a 2D planar structure.

Intuitively, $Au_5P^-$ appears difficult to obtain from $Au_4P^-$ (I), but can easily be achieved by the addition of another 2nd gold atom to $Au_4P^-$ (II). Here, although $Au_4P^-$ (II) has a significant energy difference (0.821 eV) relative to $Au_4P^-$ (I) and is not the stable structure of $Au_4P^-$, it is a possible precursor for the formation of $Au_5P^-$.

The $C_s$ structure of $Au_6P^-$ (I) is obtained by the addition of a 4th gold atom to the phosphorus atom of $Au_5P^-$. Simultaneously, a small amount of $Au_6P^-$ (II) in which the 4th gold atom binds with the 2nd and 3rd gold atoms also could be formed, as shown in Fig. 9. Similar to the $Au_5P^-$ cluster, $Au_7P^-$ does not evolve directly from the global minimum (Isomer I) of $Au_6P^-$ but instead from $Au_6P^-$ (II), with one more gold atom bonding with the 1st and 2nd gold atoms of $Au_6P^-$ (II). Further, to do so, both the 1st–1st and 1st–3rd Au–Au bonds must be broken, because of the molecular interaction forces present between the phosphorus atom and the gold atoms.

As discussed in Section 3.1, three possible stable isomers are obtained for the $Au_8P^-$ cluster. In Fig. 9, the isomer with the simplest structure was chosen for better observation of the evolutionary process. This structure is formed by the addition of a 5th gold atom to the phosphorus atom of $Au_7P^-$. Both other stable isomers of $Au_8P^-$, which are not shown in Fig. 9, can be easily obtained from this isomer by atomic interaction alone.

For the $Au_nP^-$ clusters studied, a phenomenon that also should be considered is the alternating 2D–3D geometric symmetry of the global minimum structures. As seen from Fig. 9, clusters with odd numbers of gold atoms tend to yield planar 2D

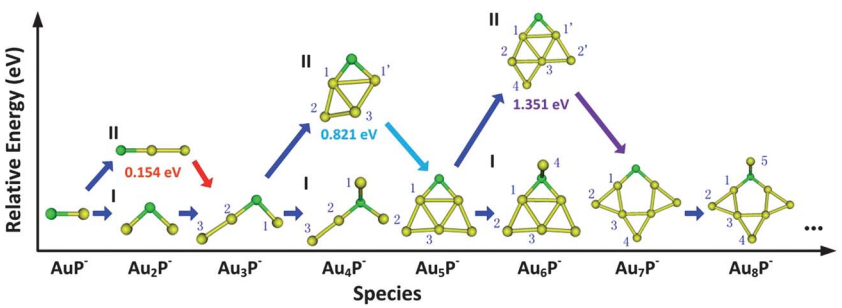


**Fig. 9** Structural evolution of $Au_nP^-$ ($n$ = 1–8).

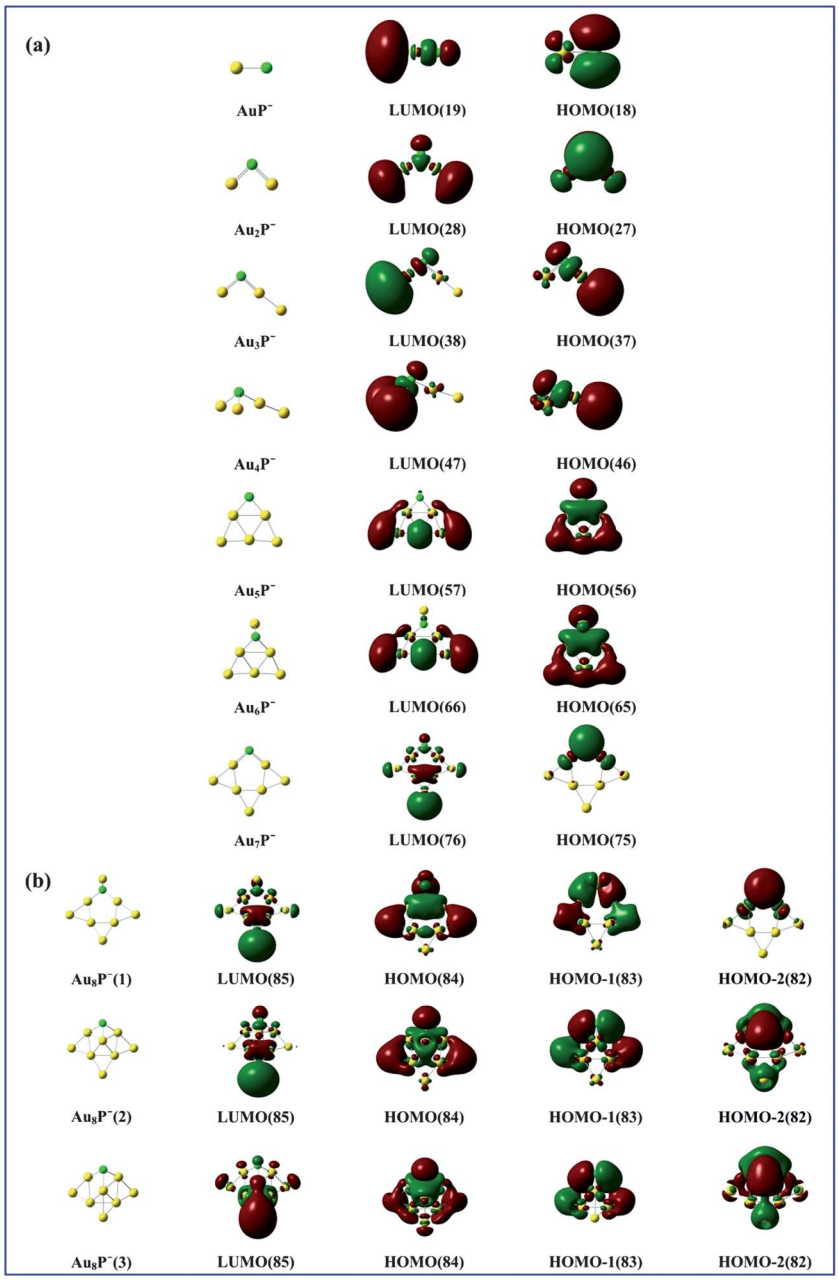


**Fig. 10** The frontier molecular orbitals of (a) $Au_nP^-$ ($n$ = 1–7) and (b) $Au_8P^-$ with three isomers. The figures in brackets represent the number of molecular orbitals.

structures, while clusters with even numbers of gold atoms tend to give 3D structures. It also can be seen that clusters in which phosphorus bonds with two gold atoms exhibit 2D configurations with the anion owning an even number of electrons (*i.e.*, obtaining a closed shell); in contrast, the clusters tend to form 3D configurations (*i.e.*, open shells) when the phosphorus bonds with three gold atoms. For $Au_3P^- \rightarrow Au_4P^-$, $Au_5P^- \rightarrow Au_6P^-$, and $Au_7P^- \rightarrow Au_8P^-$, as an additional gold atom is added to the phosphorus atom of the former cluster in each group, the structure of the cluster transforms from a 2D planar structure to a 3D configuration. The reason for this parity phenomenon may reside in the difference between the outer-shell electrons, for which $Au_nP^-$ ($n$ = 3, 5, 7) has an odd number of electrons while $Au_nP^-$ ($n$ = 2, 4, 6, 8) owns an even number. The similarity of PES for even and odd numbers of gold atoms also indicates that two branches of structural evolution paths exist.

### 3.4 Molecular orbital analysis

To understand further the evolution of $Au_nP^-$ ($n$ = 1–8), several molecular orbitals of the species were investigated. Fig. 10 shows the frontier molecular orbits of the global minimum of each species of $Au_nP^-$ ($n$ = 1–7) (a) and the LUMO and the first three molecular orbits of the three low-lying energetic isomers of $Au_8P^-$ (b). Some of the information gleaned from the figures is listed below.

(1) $AuP^-$ & $Au_2P^-$, $Au_3P^-$ & $Au_4P^-$, $Au_5P^-$ & $Au_6P^-$, $Au_7P^-$ & $Au_8P^-$ can be treated as four groups, because each has similar LUMO and HOMO values (more orbital information can be obtained from Fig. S9†). This indicates that the clusters of each group have similar orbital types. The precursor cluster to each group is an open shell, and the latter has an additional gold atom and is a closed shell, which has additional outer electrons. Hence, it is straightforward to evolve from an open-shell cluster to a closed-shell cluster with minimal changes identified using molecular orbital theory.

(2) It was found that open-shell clusters, such as $Au_nP^-$ ($n$ = 1, 3, 5, 7), add 9 molecular orbits to the closed-shell clusters, *i.e.*, $Au_nP^-$ ($n$ = 2, 4, 6, 8). In contrast, 10 orbits are added when from a closed-shell transitions to an open-shell structure. It is known that gold atoms share the $6s^1$ atomic orbital. The single outside electron can combine with the open-shell orbital to form a close-shell orbital when a gold atom is added to the open-shell cluster, achieving $Au_nP^-$ ($n$ = 1, 3, 5, 7). This reduces one occupied molecular orbital.

The LUMO and first three molecular orbitals of the three isomers of $Au_8P^-$ are plotted in Fig. 10b. The three isomers show similar orbital character. However, comparing the first four MOs of $Au_7P^-$ (see Fig. S9†) to that of $Au_8P^-$, two different bonding characters can be associated with the occupied HOMO and HOMO−1, causing the HOMO of $Au_8P^-$ (1) (as well as that of $Au_8P^-$ (2) and $Au_8P^-$ (3)) to differ from the HOMO of $Au_7P^-$, as exhibited by the former three groups. This may be due to the relativistic effects of gold atoms, which influence the hybridisation orbits of $Au_8P^-$ relative to that of $Au_7P^-$, as a result of the increase of one gold atom. The relativistic effects lower the energy of the 6s orbital of the gold atom, bringing it closer to the energy of the 5d orbital. With an increasing number of gold atoms, the relativistic effects finally cause a distinguishable difference in the MO reversion.

## 4. Conclusion

We presented a theoretical study of the structural and electronic effects of doping clusters in the size range of 1–8 atoms. It was found that the structures of $Au_nP^-$ clusters have one global minimum structure for $n \leq 7$, while $Au_8P^-$ gives 3 global minima, based on the different theoretical methods used. The principle of evolution of the $Au_nP^-$ clusters showed different growth paths relative to that of pure gold clusters or gold clusters doped with other elements because of the unique character of triple outer 3p electrons in phosphorus. Clusters with odd numbers of gold atoms tend to yield planar 2D structures, while clusters with even numbers of gold atoms tend to give 3D structures. This study elucidates the structures of $Au_nP^-$ clusters and gives the theoretical simulated photoelectron spectra. The phosphorus dopant used can modify the structure of the clusters, and shows parity on the evolutionary path from a small cluster to a medium cluster.

Experimental knowledge of phosphorus-doped clusters remains necessary for determining their sizes and shapes. In our future work, we will investigate medium- to large-size phosphorus-doped clusters.

## Acknowledgements

The theoretical work was supported by the National Natural Science Foundation of China (Grant no. 21073196), the State Key Program of the National Natural Science of China (Grant no. 21133008), the Director Foundation of AIOFM (Grant No. Y23H161131 and Y03AG31146), and CAS. A portion of the computational work was performed at the Supercomputing Center of the Chinese Academy of Sciences and the Supercomputing Center of USTC.

## References

1 P. Pyykkö, *Angew. Chem., Int. Ed.*, 2004, **43**, 4412.
2 P. Pyykkö, *Inorg. Chim. Acta*, 2005, **358**, 4113.
3 P. Pyykkö, *Chem. Soc. Rev.*, 2008, **37**, 1967.
4 M. Haruta, *Catal. Today*, 1997, **36**, 153.
5 A. A. Herzing, C. J. Kiely, A. F. Carley, P. Landon and G. J. Hutchings, *Science*, 2008, **321**, 1331.
6 H. Häkkinen, M. Moseler and U. Landman, *Phys. Rev. Lett.*, 2002, **89**, 033401.
7 F. Furche, R. Ahlrichs, P. Weis, C. Jacob, S. Gilb, T. Bierweiler and M. M. Kappes, *J. Chem. Phys.*, 2002, **117**, 6982.
8 H. Häkkinen, B. Yoon, U. Landman, X. Li, H. J. Zhai and L. S. Wang, *J. Phys. Chem. A*, 2003, **107**, 6168.
9 S. Bulusu, X. Li, L. S. Wang and X. C. Zeng, *Proc. Natl. Acad. Sci. U. S. A.*, 2006, **103**, 8326.
10 X. Xing, B. Yoon, U. Landman and J. H. Parks, *Phys. Rev. B: Condens. Matter Mater. Phys.*, 2006, **74**, 165423.
11 J. Li, X. Li, H. J. Zhai and L. S. Wang, *Science*, 2003, **299**, 864.
12 P. Gruene, D. M. Rayner, B. Redlich, A. F. G. van der Meer, J. T. Lyon, G. Meijer and A. Fielicke, *Science*, 2008, **321**, 674.
13 B. Yoon, P. Koskinen, B. Huber, O. Kostko, B. von Issendorff, H. Häkkinen, M. Moseler and U. Landman, *ChemPhysChem*, 2007, **8**, 157.
14 S. Bulusu, X. Li, L. S. Wang and X. C. Zeng, *J. Phys. Chem. C*, 2007, **111**, 4190.
15 M. Ji, X. Gu, X. Li, X. G. Gong, J. Li and L. S. Wang, *Angew. Chem., Int. Ed.*, 2005, **44**, 7119.
16 A. F. Jalbout, F. F. Contreras-Torres, L. A. Perez and I. L. Garzon, *J. Phys. Chem. A*, 2008, **112**, 353.
17 A. Lechtken, D. Schooss, J. R. Stairs, M. N. Blom, F. Furche, N. Morgner, O. Kostko, B. von Issendorff and M. M. Kappes, *Angew. Chem., Int. Ed.*, 2007, **46**, 2944.
18 X. Gu, S. Bulusu, X. Li, X. C. Zeng, J. Li, X. G. Gong and L. S. Wang, *J. Phys. Chem. C*, 2007, **111**, 8228.
19 I. E. Santizo, F. Hidalgo, L. A. Pérez, C. Noguez and I. L. Garzón, *J. Phys. Chem. C*, 2008, **112**, 17533.
20 I. L. Garzón, K. Michaelian, M. R. Beltran, A. Posada-Amarillas, P. Ordejón, E. Artacho, D. Sánchez-Portal and J. M. Soler, *Phys. Rev. Lett.*, 1998, **81**, 1600.
21 H. Häkkinen, M. Moseler, O. Kostko, N. Morgner, M. A. Hoffmann and B. von Issendorff, *Phys. Rev. Lett.*, 2004, **93**, 093401.
22 W. Huang, M. Ji, C. D. Dong, X. Gu, L. M. Wang, X. G. Gong and L. S. Wang, *ACS Nano*, 2008, **2**, 897.

 

23 N. Shao, W. Huang, Y. Gao, L. M. Wang, X. Li, L. S. Wang and X. C. Zeng, *J. Am. Chem. Soc.*, 2010, **132**, 6596.
24 W. Bouwen, F. Vanhoutte, F. Despa, S. Bouckaert, S. Neukermans, L. T. Kuhn, H. Weidele, P. Lievens and R. E. Silverans, *Chem. Phys. Lett.*, 1999, **314**, 227.
25 M. Heinebrodt, N. Malinowski, F. Tast, W. Branz, I. M. L. Billas and T. P. Martin, *J. Chem. Phys.*, 1999, **110**, 9915.
26 K. Koyasu, M. Mitsui, A. Nakajima and K. Kaya, *Chem. Phys. Lett.*, 2002, **358**, 224.
27 B. R. Sahu, G. Maofa and L. Kleinman, *Phys. Rev. B: Condens. Matter Mater. Phys.*, 2003, **67**, 115420.
28 K. Koszinowski, D. Schröder and H. Schwarz, *ChemPhysChem*, 2003, **4**, 1233.
29 H. Häkkinen, W. Abbet, A. Sanchez, U. Heiz and U. Landman, *Angew. Chem., Int. Ed.*, 2003, **42**, 1297.
30 E. Janssens, H. Tanaka, S. Neukermans, R. E. Silverans and P. Lievens, *New J. Phys.*, 2003, **5**, 46.
31 H. Tanaka, S. Neukermans, E. Janssens, R. E. Silverans and P. Lievens, *J. Am. Chem. Soc.*, 2003, **125**, 2862.
32 L. Gagliardi, *J. Am. Chem. Soc.*, 2003, **125**, 7504.
33 H. Tanaka, S. Neukermans, E. Janssens, R. E. Silverans and P. Lievens, *J. Chem. Phys.*, 2003, **119**, 7115.
34 H. J. Zhai, J. Li and L. S. Wang, *J. Chem. Phys.*, 2004, **121**, 8369.
35 E. Janssens, H. Tanaka, S. Neukermans, R. E. Silverans and P. Lievens, *Phys. Rev. B: Condens. Matter Mater. Phys.*, 2004, **69**, 085402.
36 D. W. Yuan, Y. Wang and Z. Zeng, *J. Chem. Phys.*, 2005, **122**, 114310.
37 M. B. Torres, E. M. Fernandez and L. C. Balbas, *Phys. Rev. B: Condens. Matter Mater. Phys.*, 2005, **71**, 115412.
38 H. Wen, Y. R. Liu, T. Huang, K. M. Xu, W. J. Zhang, W. Huang and L. S. Wang, *J. Chem. Phys.*, 2013, **138**, 174303.
39 E. J. Fernández, A. Laguna and M. E. Olmos, *J. Chil. Chem. Soc.*, 2007, **52**, 1200.
40 A. I. Kozlov, A. P. Kozlova, H. C. Liu and Y. Iwasawa, *Appl. Catal., A*, 1999, **182**, 9.
41 W. Jeitschko and M. H. Möller, *Acta Crystallogr., Sect. B: Struct. Crystallogr. Cryst. Chem.*, 1979, **35**, 573.
42 M. Eschen and W. Jeitschko, *J. Solid State Chem.*, 2002, **165**, 238.
43 V. G. Weizer and N. S. Fatemi, *J. Appl. Phys.*, 1991, **69**, 8253.
44 A. E. Henkes, Y. Vasquez and R. E. Schaak, *J. Am. Chem. Soc.*, 2007, **129**, 1896.
45 Z. Y. Liu, R. B. Huang and L. S. Zheng, *Chem. Res. Chin. Univ.*, 1997, **18**, 293.
46 N. R. Panyala, E. M. Peña-Méndez and J. Havel, *Rapid Commun. Mass Spectrom.*, 2012, **26**, 1100.
47 X. D. Wen, T. J. Cahill and R. Hoffmann, *J. Am. Chem. Soc.*, 2009, **131**, 2199.
48 Y. Li, Y. P. Cao, Y. F. Li, S. P. Shi and X. Y. Kuang, *Eur. Phys. J. D*, 2012, **66**, 10.
49 G. F. Zhao, Y. L. Wang, J. M. Sun and Y. X. Wang, *Acta Phys.-Chim. Sin.*, 2012, **28**, 1355.
50 M. Zhang, S. Chen, Q. M. Deng, L. M. He, L. N. Zhao and Y. H. Luo, *Eur. Phys. J. D*, 2010, **58**, 117.
51 C. Majumder, A. Kandalam and P. Jena, *Phys. Rev. B: Condens. Matter Mater. Phys.*, 2006, **74**, 205437.
52 S. H. Yoo and X. C. Zeng, *Angew. Chem., Int. Ed.*, 2005, **44**, 1491.
53 D. J. Wales and J. P. K. Doye, *J. Phys. Chem. A*, 1997, **101**, 5111.
54 W. Huang, R. Pal, L. M. Wang, X. C. Zeng and L. S. Wang, *J. Chem. Phys.*, 2010, **132**, 054305.
55 S. Yoo and X. C. Zeng, *J. Chem. Phys.*, 2003, **119**, 1442.
56 J. P. Perdew, K. Bruke and M. Ernzerhof, *Phys. Rev. Lett.*, 1996, **77**, 3865.
57 A. D. Becke, *J. Chem. Phys.*, 1993, **98**, 5648.
58 C. T. Lee, W. T. Yang and R. G. Parr, *Phys. Rev. B: Condens. Matter Mater. Phys.*, 1988, **37**, 785.
59 A. D. Becke, *Phys. Rev. A: At., Mol., Opt. Phys.*, 1988, **38**, 3098.
60 R. A. Kendall, E. Apra, D. E. Bernholdt, E. J. Bylaska, M. Dupuis, G. I. Fann, R. J. Harrison, J. L. Ju, J. A. Nichols, J. Nieplocha, T. P. Straatsma, T. L. Windus and A. T. Wong, *Comput. Phys. Commun.*, 2000, **128**, 260.
61 E. J. Bylaska, W. A. de Jong, N. Govind, K. Kowalski, T. P. Straatsma, M. Valiev, D. Wang, E. Apra, T. L. Windus, J. Hammond, P. Nichols, S. Hirata, M. T. Hackler, Y. Zhao, P. D. Fan, R. J. Harrison, M. Dupuis, D. M. A. Smith, J. Nieplocha, V. Tipparaju, M. Krishnan, Q. Wu, T. Van Voorhis, A. A. Auer, M. Nooijen, E. Brown, G. Cisneros, G. I. Fann, H. Fruchtl, J. Garza, K. Hirao, R. Kendall, J. A. Nichols, K. Tsemekhman, K. Wolinski, J. Anchell, D. Bernholdt, P. Borowski, T. Clark, D. Clerc, H. Dachsel, M. Deegan, K. Dyall, D. Elwood, E. Glendening, M. Gutowski, A. Hess, J. Jaffe, B. Johnson, J. Ju, R. Kobayashi, R. Kutteh, Z. Lin, R. Littlefield, X. Long, B. Meng, T. Nakajima, S. Niu, L. Pollack, M. Rosing, G. Sandrone, M. Stave, H. Taylor, G. Thomas, J. van Lenthe, A. Wong, and Z. Zhang, *NWChem, A Computational Chemistry Package for Parallel Computers, Version 5.1*, Pacific Northwest National Laboratory, Richland, 2009.
62 C. Adamo and V. Barone, *J. Chem. Phys.*, 1999, **110**, 6158.
63 R. B. Ross, J. M. Powers, T. Atashroo, W. C. Ermler, L. A. Lajohn and P. A. Christiansen, *J. Chem. Phys.*, 1990, **93**, 6654.
64 W. Huang, S. Bulusu, R. Pal, X. C. Zeng and L. S. Wang, *ACS Nano*, 2009, **3**, 1225.
65 W. Huang, S. Bulusu, R. Pal, X. C. Zeng and L. S. Wang, *J. Chem. Phys.*, 2009, **131**, 234305.
66 L. M. Wang, R. Pal, W. Huang, X. C. Zeng and L. S. Wang, *J. Chem. Phys.*, 2010, **132**, 114306.
67 R. Pal, L. M. Wang, W. Huang, L. S. Wang and X. C. Zeng, *J. Chem. Phys.*, 2011, **134**, 054306.
68 R. Pal, W. Huang, Y. L. Wang, H. S. Hu, S. Bulusu, X. G. Xiong, J. Li, L. S. Wang and X. C. Zeng, *J. Phys. Chem. Lett.*, 2011, **2**, 2288.
69 Y. F. Li, X. Y. Kuang, S. J. Wang and Y. R. Zhao, *J. Phys. Chem. A*, 2010, **114**, 11691.
70 C. J. Wang, X. Y. Kuang, H. Q. Wang, H. F. Li, J. B. Gu and J. Liu, *Comput. Theor. Chem.*, 2012, **1002**, 31.
71 B. Kiran, X. Li, H. J. Zhai, L. F. Cui and L. S. Wang, *Angew. Chem., Int. Ed.*, 2004, **43**, 2125.

72 Y. L. Cao, C. van der Linde, R. F. Hockendorf and M. K. Beyer, *J. Chem. Phys.*, 2010, **132**, 224307.
73 H. Häkkinen and U. Landman, *Phys. Rev. B: Condens. Matter Mater. Phys.*, 2000, **62**, R2287.
74 Y. C. Lin and D. Sundholm, *J. Phys. Chem. A*, 2012, **116**, 5119.
75 R. Pal, L. M. Wang, W. Huang, L. S. Wang and X. C. Zeng, *J. Am. Chem. Soc.*, 2009, **131**, 3396.

 